Extended Morse Function Model for Angle-Dependent Hydrogen Bond in Protein−Protein Interactions

Hwanho Choi,[†] Hongsuk Kang,[†,‡] and Hwangseo Park*

Department of Bioscience and Biotechnology, Sejong University, 98 Kunja-Dong, Kwangjin-Ku, Seoul 143-747, Korea.

Received: October 19, 2009; Revised Manuscript Received: December 11, 2009

Backbone−backbone, backbone−asparagine, and serine−backbone hydrogen bonds (HBs) are the most abundant interactions at the interface of protein−protein complex. Here, we propose an angle-dependent potential energy function for these HBs constructed by the product of the radial and the angular Morse functions whose various parameters are optimized with high-level density functional theory (DFT) calculations. The new angular variables, the interatomic distance between the donor and the acceptor atoms (R_θ) and that between the hydrogen and the base atom of the acceptor (R_ϕ), are employed to define the angular Morse functions. The angular part in the new potential function is found to be comparable in the magnitude of energy values to the radial one, which is consistent with the significant angular dependence of HBs. The HB binding energies calculated with the new potential function compare well with those obtained by high-level DFT calculations with the associated squared correlation coefficients ranging from 0.82 to 0.85. This agreement indicates the suitability of the new energy functions as a potential function for HB in modeling the protein−protein interactions.

Introduction

Protein−protein interactions (PPIs) serve as the physical basis of biological signaling. In the subtle regulations of biological systems, the intermolecular hydrogen bonds (HBs) make a significant contribution to the stability the protein−protein complex. Because the identification of the interacting partners for a given protein can provide valuable information about its detailed role in biological processes,[1] many experimental and computational efforts have been devoted to the development of a reliable method to predict the interacting protein partners of a protein of interest. Several high-throughput experimental techniques including the yeast two-hybrid method,[2] the identification by mass spectrometry of isolated protein complexes,[3] and the protein chips[4] proved to be successful in identifying the interacting domains, which has led to the establishment of several databases for PPI prediction.[5–7] Supplementary to these useful experimental approaches, several computational methods have also been developed to improve the reliability of the results from the comprehensive high-throughput PPI predictions.[8,9]

Nonetheless, the development of an accurate potential energy function of HBs has lagged behind the successful description of the structural features of HBs established in a variety of forms. Such a difficulty in quantitative theoretical modeling of HB stems from the diversity in its energy components including electrostatic, exchange repulsion, charge transfer, and polarization interaction energies. Earlier studies have shown that the individual energy ingredients of HB can be estimated with the decomposition analysis of the interaction energy based on quantum chemical calculations. The methods for HB energy decomposition include the reduced variational space self-consistent (RVS SCF)[10] and Kitaura-Morokuma (KM)[11] methods. The related quantum chemical investigations showed that in addition to the electrostatic energy contribution, the charge-transfer interaction from a nonbonding orbital of the acceptor atom to the antibonding σ^* molecular orbital of the donor group should also be a significant ingredient of the HB binding energy.[12,13] Because the strength of such a charge-transfer interaction depends on the orientation of the donor and acceptor groups, a proper potential energy function for HBs should include the angular term to penalize the geometry unfavorable for the charge-transfer interaction. In this regard, an HB potential has been proposed that consists of the Leonard-Jones (LJ) 12-10 potential as a radial part and the angular part of various trigonometric functions with respect to the donor-hydrogen-acceptor and the hydrogen-donor-base angles.[14] This function has proved to be useful as an HB energy function for the intra- and intermolecular interactions of a protein.[15,16] However, it needs to be modified because the statistical analysis of the crystal structures indicated the existence of some excluded regions associated with the angular dependence of HB at the interface of PPI.[17–24]

In the previous work, we proposed an angle-dependent potential energy function for backbone (Bck)−backbone (Bck) HB at the interface of PPI, which comprises the Morse potential and the product of the power series of sine and cosine functions as the radial and the angular parts, respectively.[25] This new HB potential function compared reasonably well with the knowledge-based potential derived by applying Boltzmann statistics for a variety of protein−protein complexes in protein data bank (PDB) as well as with the energetic and structural features of the Bck−Bck HB obtained from high-level quantum chemical calculations. The present study is aimed to suggest a new potential energy function and the associated energy parameters for the most abundant HBs at the interface of PPI. More specifically, we will address the suitability of a multidimensional Morse function and the associated optimized parameters in modeling Bck−Bck, Bck−asparagine/glutamine (Asn), and serine/threonine (Ser)−Bck HBs. For this purpose, the extensive density functional theory (DFT) calculations are carried out on

* To whom correspondence should be addressed. Telephone: +82-2-3408-3766. Fax: +82-2-3408-4334. E-mail: hspark@sejong.ac.kr.
† Both authors equally contributed to this work.
‡ Current address: Chemical Physics Program, University of Maryland, College Park, MD 20742.

10.1021/jp909983y
Published on Web 02/08/2010

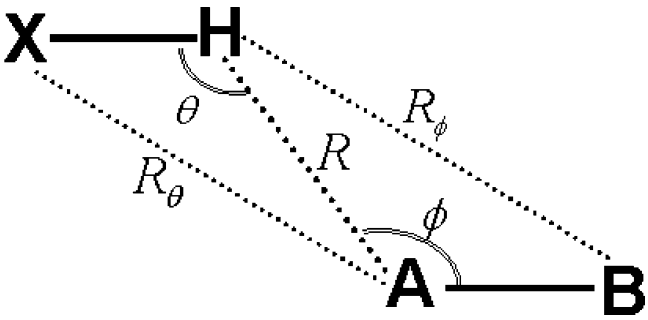

Figure 1. The coordinate system and the geometrical variables for the definition of an HB potential energy function. R is the HB distance while θ and ϕ are the angles formed by the two donor and one acceptor atoms, and that of the two acceptor and one donor atoms, respectively. R_θ and R_ϕ are the interatomic distances associated with the two HB angles.

the relevant model systems for the three HBs. The potential energy function and the associated energy parameters in the radial and the angular parts are derived in such a way that minimizes the difference between the DFT binding energies and the estimated HB potential energies. It will be shown that the newly obtained potential energy function would be more suitable than the previous ones in elucidating the energetic and structural features of the HBs at the interface of PPI.

Theory and Computational Methods

Theoretical Modeling of HB. A useful coordinate system for describing HB is illustrated in Figure 1. At least three geometrical variables are required for the HB established in the form of X−H···A−B.[26,27] Included in these variables are the HB distance (R), the angle formed by the two donor and one acceptor atoms (θ), and that of the two acceptor and one donor atoms (ϕ). θ and ϕ can serve as useful variables when the radial and the angular contributions of HB energy are mutually independent. Two other angular parameters, the interatomic distance between the donor and the acceptor atoms (R_θ) and that between the hydrogen and the base atom of the acceptor (R_ϕ), may be more suitable than θ and ϕ for describing the HBs in which the radial contribution has a significant effect on the angular one because they increase and decrease in the same way as R as well as θ and ϕ.

Within the coordinate system in Figure 1, the potential energy function for HB can be expressed as the product of the radial and the angular parts

$$V_{\mathrm{HB}}(R,\theta,\phi) = f(R)g(\theta,\phi) \tag{1}$$

LJ 12-10 potential was most widely used as the radial part of HB energy function because it is appropriate for describing the nonbonding nature of HB interaction. However, this function has proved to be inappropriate to model the HB due to the inherence of some covalent character in most of HBs. The covalent contribution is important especially when the electron cloud on the nonbond orbital of the acceptor atom transfers to the σ^* orbital of the X−H bond to a significant extent. In this case, Morse function can be an alternative for the radial part because it has been shown to properly model a covalent bond with anharmonicity[28,29]

$$f(R) = D_{\mathrm{e}}(1 - e^{-\alpha(R-R_0)})^2 \tag{2}$$

where D_{e} is the well depth of the potential energy and α is a measure of the curvature of $f(R)$.

The angular part of the HB potential has often been described by sine and cosine functions with respect to θ and ϕ angles and their power series. However, the periodicity of these angular functions has limited the accuracy of the potential function because of the difficulty in considering the geometrically forbidden region in the formation of HB. Furthermore, it is difficult to obtain the associated potential parameters in such angular functions due to a bad convergence during the optimization. Therefore, we introduce a new angular function that can effectively penalize the geometry unfavorable for the formation of HB at the interface of PPI. As in the radial part, the new angular functions have a form of Morse function with respect to the new angular variables, R_θ and R_ϕ. The reason for the choice of Morse function lies in that the angular distributions of HB in PPI have revealed a similarity to a Morse function.[20,30] The angular part of the HB potential can thus be written as follows

$$g(R_\theta, R_\phi) = D_{\theta\phi}(1 - \exp[-\vec{\mathbf{a}}\cdot\vec{\mathbf{R}}_{\theta\phi}])^2 \tag{3}$$

Here, $\vec{\mathbf{a}}$ and $\vec{\mathbf{R}}_{\theta\phi}$ are the vectors of the exponents and the displacements for the two angular parameters, respectively

$$\vec{\mathbf{a}} = (a_\theta, a_\phi) \text{ and } \vec{\mathbf{R}}_{\theta\phi} = (R_\theta - R_\theta^0, R_\phi - R_\phi^0) \tag{4}$$

It should be noted that the angular dependency of the HB energy function diminishes with the increase of R and vanishes beyond the HB defining distance. This indicates that the angular function should it itself have a functional dependence on R. Therefore, the parameters in the angular function should be expressed as a function of R. We assume in this regard that the exponents and the equilibrium distances in the angular Morse function would be expressed as Morse and linear functions, respectively, with respect to R as follows

$$a_\theta = D_\theta(1 - \exp[-\beta_\theta(R - R_{a\theta}^0)])^2 \text{ and } a_\phi = D_\phi(1 - \exp[-\beta_\phi(R - R_{a\phi}^0)])^2 \tag{5}$$

$$R_\theta^0 = A_\theta R + B_\theta \text{ and } R_\phi^0 = A_\phi R + B_\phi \tag{6}$$

Finally, 10 parameters in eqs 5 and 6 are subject to be optimized in such a way as to minimize the difference between the DFT binding energies and the potential energies calculated in a variety of HB configurations.

Calculation of ab initio Potential Energy Landscapes. Bck−Bck, Bck−Asn, and Ser−Bck HBs have been shown to be the most abundant interactions at the interface of PPI.[25] To obtain a baseline to optimize the parameters in the HB energy function, the potential energy landscapes of the three HBs were probed through the partial geometry optimizations on the relevant model systems with the latest version of GAMESS code.[31] These quantum chemical geometry optimizations were carried out based on the DFT calculations with 6-311G** basis set for all atoms. The B3LYP hybrid density functional was employed for all calculations. This functional consists of Becke's hybrid gradient-corrected exchange functional[32] and the gradient-corrected correlation functional of Lee, Yang, and Parr.[33] The reason for the choice of DFT rather than the Hartree−Fock method in this study lies in that the latter is known to underestimate the

binding energies of HB complexes due to the neglect of electron correlation effects. The sum of the energies of the isolated donor and acceptor was taken as the reference to calculate the binding energy in a given HB configuration.

As widely used in the other studies,[12,34] *N*-methylacetamide (NMA), acetamide, and methanol were selected as the simplified structural models for backbone amide group, and the side chains of asparagine (glutamine) and serine (threonine), respectively. To estimate the energy landscapes for the three HBs under investigation, we calculated the binding energies on the partially optimized NMA dimer, and NMA−acetamide and methanol−NMA complexes with varying R, R_θ, and R_ϕ values by the step of 0.1 Å. In calculating the binding energy for a given HB configuration, the counterpoise method was used to correct the basis set superposition error.[35]

Derivation of the Knowledge-Based HB Potential from PDB Statistics. To obtain a distribution of geometrical variables associated with the HBs at the interface of PPI, we selected 10646 protein−protein complexes from Dunbrack's culled PDB database (http://dunbrack.fccc.edu). This database lists only the crystal structures of proteins with a resolution higher than 2.0 Å. Furthermore, the proteins with the amino acid sequences homologous to the existing ones are excluded in the database, which has an effect of removing the structural redundancies in the database. For the selected crystal structures, hydrogen atoms were added according to the CHARMM22 topology parameters.[36] Each protein−protein complex was then checked for the presence of HB between the two protein motifs at the interface, which was followed by the calculation of the structural parameters illustrated in Figure 1.

To derive a knowledge-based potential function to describe the HB at the interface of PPI, we assumed that the HB energies should follow a Boltzmann distribution with respect to the populations of the three structural parameters. Within the framework of this Boltzmann statistics, the probability that the HB established with the structural parameters R, R_θ, and R_ϕ can be related with how frequently the HB with the given parameter values appears in the protein data set for PPI. Thus, we have[30]

$$E(R, R_\theta, R_\phi) = -k_B T \ln \frac{\rho(R, R_\theta, R_\phi)}{\rho_{ref}(R, R_\theta, R_\phi)} \quad (7)$$

Here, k_B and T are Boltzmann constant and room temperature, respectively. $\rho(R, R_\theta, R_\phi)$ is the probability density in a Boltzmann-like expression and measures the frequency at which the three structural parameters associated with an HB are observed in the protein data set for PPI, while $\rho_{ref}(R, R_\theta, R_\phi)$ is a reference frequency assuming an unbiased distribution in the protein data set that can ensure a proper normalization of the probabilities. Thus, the energy minimum located using the knowledge-based HB potential corresponds to the most frequently observed HB in the data set. The HB defining distance between the donor and the acceptor atoms in the crystal structures were chosen to be 3.5 Å, a generally accepted distance limit for HB with moderate strength.[37] The empirical HB potential obtained from Boltzmann statistics seems to be more accurate than the HB potential function optimized based on the DFT calculations because the former is derived under consideration of the effects of the macromolecular protein structures. However, only the radial part of the empirical function can be derived at the present because the amount of PDB data for PPI is insufficient to obtain the sufficient populations for the HB angles outside the most probable ones.

Calculation of the HB Energy Parameters. Various parameters in the radial and the angular parts of the HB energy function were optimized using the calculated DFT binding energies. In this parameter optimization, Levenberg−Marquardt algorithm was employed for the gradient-based minimization on the error hypersurface (F).[38,39] This hypersurface is defined by the sum of the absolute values of the differences between the DFT binding energies (BE^{DFT}) and the HB potential energies (V_{HB}) calculated with the same structural variables

$$F = \sum_k |BE^{DFT}(R_k, R_{\theta k}, R_{\phi k}) - V_{HB}(R_k, R_{\theta k}, R_{\phi k})| \quad (8)$$

Results and Discussion

As widely employed in the other studies, NMA, acetamide, and methanol were selected as the simplified structural models for the backbone amide group, and the side chains of asparagine (glutamine) and serine (threonine), respectively. These residues were shown to be observed most frequently at the interface of PPI.[25] Figure 2 displays the geometries of NMA dimer, and NMA-acetamide and methanol-NMA complexes that were fully optimized at B3LYP/6-311G** level of theory. Consistent with the similar pK_a values for the amide and the hydroxy groups, the equilibrium hydrogen bond distances (R_0) appear to be the same for the three optimized structures. We note that this common R_0 value (1.91 Å) is within the distance range of HB with moderate strength suggested by Jeffrey,[37] and are similar to the equilibrium HB distance in the LJ 12-10 potential to describe the HBs.[16] It is also noteworthy that the optimized R_θ and R_ϕ values decrease with the change of the HB donor from the amide to the hydroxy groups. This stems from the bending of the donor−hydrogen−acceptor angle (θ) from 180°, which indicates the decrease in the extent of the charge transfer from the nonbonding orbital of the acceptor atom to the σ^* molecular orbital of the donor group. Such a decrease in charge transfer can be attributed to the higher energy of the σ^* molecular orbital for O−H bond than that for N−H one. As indicated in Figure 2, the R, R_θ, and R_ϕ values in the optimized structures compare well with the corresponding most frequently observed values in the protein data set of PPI. This supports the suitability of using B3LYP/6-311G** level of theory for modeling the three HBs abundant at the interface of PPI. Therefore, the B3LYP/6-311G** results for the structural and energetic features of the relevant model systems for the three HBs with varying R, R_θ, and R_ϕ values are used in this study as a baseline to assess the accuracies of HB potential functions and to optimize their energy parameters.

In the PDB data set for PPI, the R, R_θ, and R_ϕ values for most of the HB configurations are concentrated between 1.6 and 2.1 Å, between 2.7 and 3.0 Å, and between 2.9 and 3.2 Å, respectively, which prevents us from obtaining the reliable empirical binding energies beyond the ranges. Although the HB distances are relatively well-distributed so as to produce the radial part of empirical potential function with Boltzmann statistics, the ranges of the angular parameters are too narrow to derive the angle-dependent empirical potential functions. Thus, only the radial part of the HB potential could actually be obtained with the knowledge-based empirical methods. In this regard, high-level quantum chemical calculations with varying the radial and the angular parameters can serve as an alternative to provide a baseline to derive the angle-dependent HB potentials.

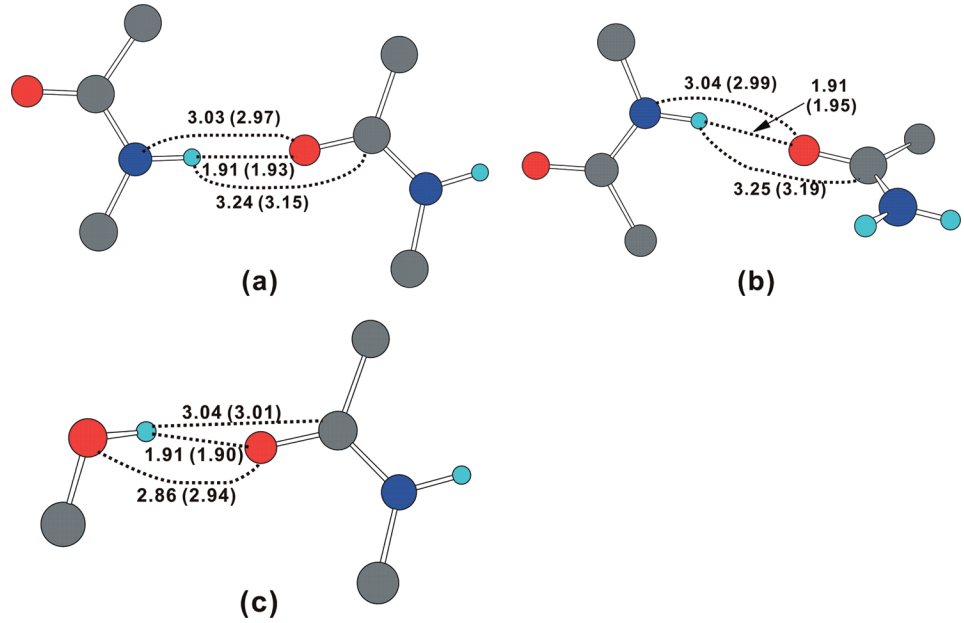

Figure 2. The structures of (a) NMA dimer, (b) NMA-acetamide, and (c) methanol-NMA complexes optimized at B3LYP/6-311G** level of theory. Equilibrium distances are indicated in Å. Numbers in parentheses are the most frequently observed distances for the corresponding HBs in the protein data set of PPI.

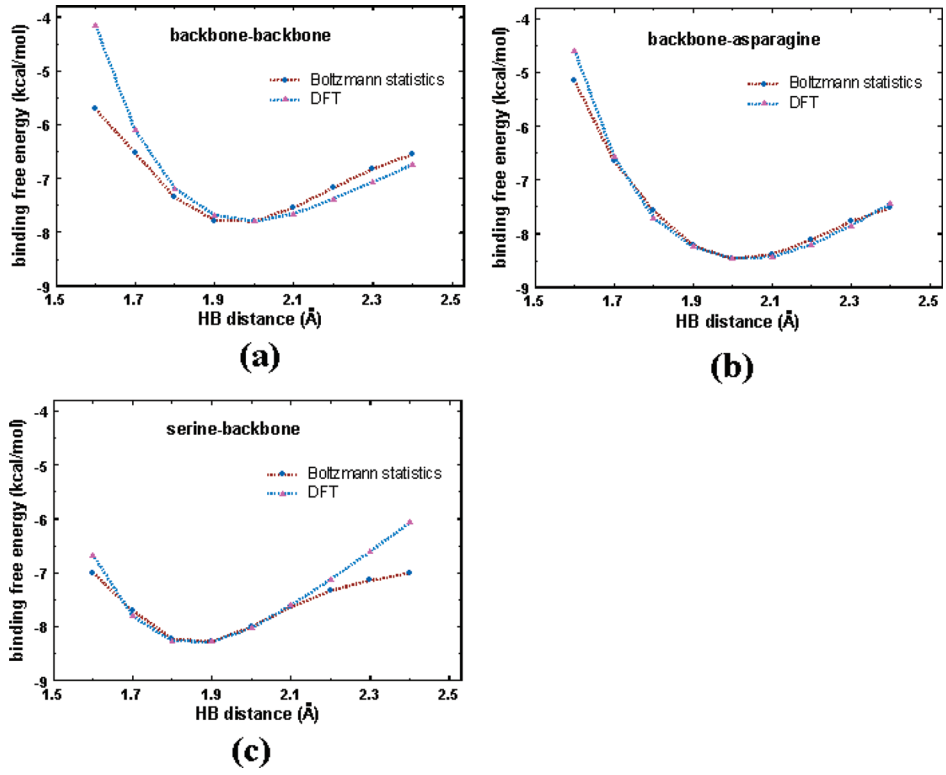

Figure 3. Comparison of the dependences of the binding free energies on the HB distance obtained from DFT calculations and Boltzmann statistics for (a) Bck−Bck, (b) Bck−Asn, and (c) Ser−Bck HBs.

Compared in Figure 3 are the dependences of the binding free energies on R values for the three HBs under investigation that were obtained from DFT calculations and Boltzmann statistics. In all three cases, both of the functional shapes resemble a Morse potential with a large exponent because of a wide distance range of the attractive region and the lack of a sharp increase in binding free energy at the short and long HB distances. DFT calculations appear to overestimate the repulsive interaction at the short distances of Bck−Bck HB and underestimate the long-range attraction at the long HB distances of Ser−Bck HB. Nonetheless, the distance dependences of DFT binding free energies compare pretty well with those obtained from the empirical results with Boltzmann statistics: the squared correlation coefficients (R^2) amount to 0.90, 0.99, and 0.93 for Bck−Bck, Bck−Asn, and Ser−Bck HBs, respectively. Besides the narrow range of R_θ, and R_ϕ values, the positions of hydrogen atoms are absent in the protein data set for PPI, which make it difficult to derive the empirical HB potentials based on Boltzmann statistics. In this regard, DFT calculations can be useful as the reference for deriving the HB potentials due to

TABLE 1: The Optimized Parameters of Three-Dimensional Morse Functions for Bck−Bck, Bck−Asn, and Ser−Bck HBs[a]

parameter	Bck−Bck	Bck−Asn	Ser−Bck
D	−8.55	−8.51	−8.67
α	1.42	1.35	1.44
R_0	1.99	1.95	1.91
D_θ	−2.99	−2.13	−2.87
β_θ	2.14	2.16	1.81
$R^0{}_{\alpha\theta}$	1.89	1.86	1.59
D_ϕ	−6.29	−9.64	−5.08
β_ϕ	3.54	3.56	3.31
$R^0{}_{\alpha\phi}$	1.67	1.48	1.70

[a] For the identification of each parameter, see eqs 2 and 5.

TABLE 2: The Optimized Equilibrium Angular Parameters ($R^0{}_\theta$ and $R^0{}_\phi$) and the Corresponding Most Probable Values ($R^{mp}{}_\theta$ and $R^{mp}{}_\phi$) in the Protein Data Set for PPI

	Bck−Bck	Bck−Asn	Ser−Bck
$R^0{}_\theta$	$0.87R + 1.18$	$0.93R + 1.16$	$0.92R + 1.14$
$R^0{}_\phi$	$0.88R + 1.46$	$0.89R + 1.42$	$0.91R + 1.33$
$R^{mp}{}_\theta$	2.97	2.99	2.94
$R^{mp}{}_\phi$	3.15[a]	3.19[a]	3.01[a]

[a] Because of the lack of the coordinates for hydrogen atoms in PDB, the distances were calculated by adding the hydrogen atoms according to the CHARMM22 topology parameters.

the optimized positioning of hydrogen atoms as well as the accuracy in predicting binding free energies of HB complexes.

Table 1 lists the optimized parameters in the radial and the angular parts of the potential functions for the three HBs under investigation. We note that the overall well depth (D) given by the product of the radial and the angular well depths (D_e and $D_{\theta\phi}$ in eqs 2 and 3, respectively) is similar among the three HBs, which is consistent with the similarity in the pK_a values of the amidic and the hydroxy moieties. The exponent in the radial part (α) ranges from 1.35 to 1.44 Å^{-1}. These values are smaller than that for the vibrational motion of diatomic molecules (1.930 Å^{-1} for hydrogen molecule), which has the effect of broadening the potential curve at the interatomic distances flanking the energy minimum. This indicates that the Morse potential optimized in this study would have a merit for reducing the overestimation of the repulsive interactions at the short interatomic distances that has been regarded as one of the major defects for LJ potentials.[23] As can be seen in Table 1, the angular parameters in the potential functions appear to vary more significantly than the radial ones with the change of HB donor and acceptor. This is not surprising because the angular part of the HB potential function has been shown to be sensitive to the choice of a radial function.[25] Nonetheless, the three parameter sets reveal a similarity with the R^2 values ranging from 0.91 to 0.95, which indicates a strong correlation between the two selected parameter sets. The three HBs abundant at the interface of PPI can thus be described by a similar potential energy function, which is consistent with the similarity in their HB strengths.

The characteristic feature that discriminates the coordinate system for HB employed in this study from the others lies in that the angular parameters should be dependent on the associated HB distances (see Figure 1). The equilibrium parameters ($R^0{}_\theta$ and $R^0{}_\phi$) in the angular Morse function can in this regard be approximated as a linear function with respect to R. Summarized in Table 2 are the optimized linear functions of $R^0{}_\theta$ and $R^0{}_\phi$ in comparison to the corresponding most probable values ($R^{mp}{}_\theta$ and $R^{mp}{}_\phi$) in the protein data set for PPI. Incorporating the R_0 values in Table 1 into $R^0{}_\theta$ and $R^0{}_\phi$, it follows immediately that the two equilibrium angular parameters are in good agreement with the corresponding $R^{mp}{}_\theta$ and $R^{mp}{}_\phi$ values. This agreement indicates that the present coordinate system involving the distance-dependent angular variables should be useful for deriving the potential energy function and the associated parameters for the HBs abundant at the interface of PPI. A significant dependence of the angular distribution on the HB distance has also been observed in the HBs involved in the monomeric proteins[20] and the crystal structures of small-molecule dimers.[30]

Figure 4 shows the overall shapes of the optimized angular functions for the three HBs in comparison with those obtained from the B3LYP/6-311G* calculations. The optimizations of the angular functions were performed at their respective equilibrium HB distances (R_0). It is seen that the optimized angular potential functions appear to be similar in functional shape to the original angular potential energies calculated from the DFT calculations. The R^2 values between the energy values calculated from the potential function and those from DFT calculations amount to 0.90, 0.94, and 0.95 for Bck−Bck, Bck−Asn, and Ser−Bck HBs, respectively. This reproducibility of DFT results indicates the appropriateness of the employed angular variables and the functional forms to describe the HBs.

In contrast to the high similarity of the radial potential functions among the three HBs, the shapes of the three angular HB potentials appear to be quite different with the distinctive regions of energy minima. We note in this regard that whereas the equilibrium R_ϕ values ($R^0{}_\phi$) are located around 3.3 Å in all three cases, $R^0{}_\theta$ decreases in going from Bck−Bck to Bck−Asn and Ser−Bck HBs. This can be attributed to the decrease in steric hindrance due to the decrease in the number of heavy atoms. The most significant difference among the angular potentials lies in the well breadth, which indicates a large difference in the flexibilities of the three HBs. Bck−Bck HB exhibits the highest flexibility with respect to the variation of angular parameters. Because Bck−Bck HB is the most abundant interaction at the interface of PPI, its structural flexibility may be invoked to explain the plasticity inherent in PPI.[40]

In the optimized angular potentials for the three HBs, it is also noteworthy that the energy values range from −8 to −3 kcal/mol in all three cases, the minima of which are comparable to those of the radial parts amounting to 7−9 kcal/mol. This disproves the previous results that the HB potential should be dominated by the radial part with relatively insignificant contribution of the angular part.[15,25] The significance of the angular dependence in binding free energies of the HB complexes has also been well-appreciated in a variety of theoretical and experimental studies.[17,23,24,26,30,41–46] Because the angular dependence of the HB potential stems from the contribution of the charge-transfer interaction in the HB complexes, such a large contribution of the angular part indicates its importance in HBs to a comparable extent to the electrostatic interaction reflected in the radial counterpart. In this regard, the present HB potential function might be inaccurate in describing the HBs involving the charged residue(s) in which the electrostatic interaction should be a dominant ingredient of the binding energy.

Shown in Figure 5 are the correlations between the HB interaction energies calculated from B3LYP/6-311G** level of theory with varying R, R_θ, and R_ϕ values and those obtained with HB potential functions in the same HB

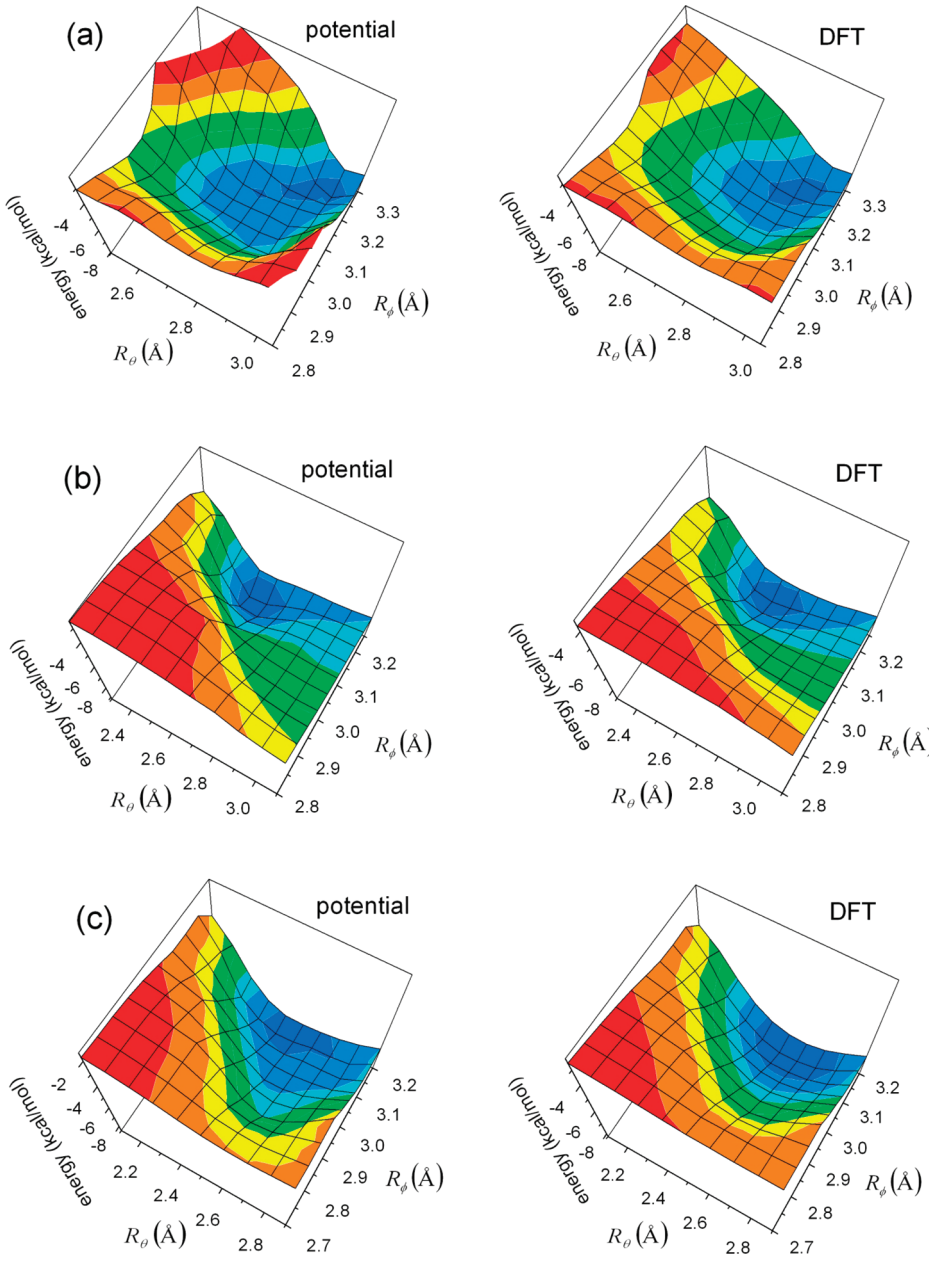

Figure 4. Comparative view of the angular potentials obtained from the optimized potential functions and DFT calculations for (a) Bck−Bck, (b) Bck−Asn, and (c) Ser−Bck HBs.

configurations. Because the DFT electronic energy is a variational quantity, the binding energies of the complexes calculated at B3LYP/6-311G** level vary very gently with the change in HB geometry. Therefore, the HB configurations with the calculated binding energy differing by more than 0.1 kcal/mol from the previous steps were selected only for estimating the correlation with the new potential energy functions for the three HBs. For the 270 HB configurations selected with the energy criterion, we obtain the R^2 values of 0.85, 0.82, and 0.84 for Bck−Bck, Bck−Asn, and Ser−Bck HBs, respectively, which indicates a strong correlation between the binding free energies obtained from DFT calculations and those from the optimized HB potential functions. It is noted that the R^2 value for the Bck−Bck HB increases from 0.81 in the previous work in which a power series of trigonometric functions was employed as the angular part of the HB. This increase in the reproducibility of DFT results indicates that the current angular potential in the form of the Morse function defined with respect to the new angular parameters should be superior to the previous one in explaining the structural and energetic features of the Bck−Bck HB in PPI. However, the fact that the correlation coefficients remain within 0.85 indicates the possibility of further improvement in accuracy, which may be attributed to the imperfect reflection of the charge redistribution from the lone pair electrons of the HB acceptor atom to the donor group. We expect in this regard that the HB potentials would become more accurate with the incorporation of an additional term to properly describe the electrostatic interactions in HB complexes involving the lone pair electrons of the HB acceptor atom.

Actually the trigonometric functions and their power series should be inappropriate for modeling the angular dependence of HBs because their nonconvergent behavior prevents the HB potential energy from vanishing at the long distances beyond the HB defining region. In contrast, Morse function can be useful for the angular part as well as the radial one because both radial and angular dependences are related with

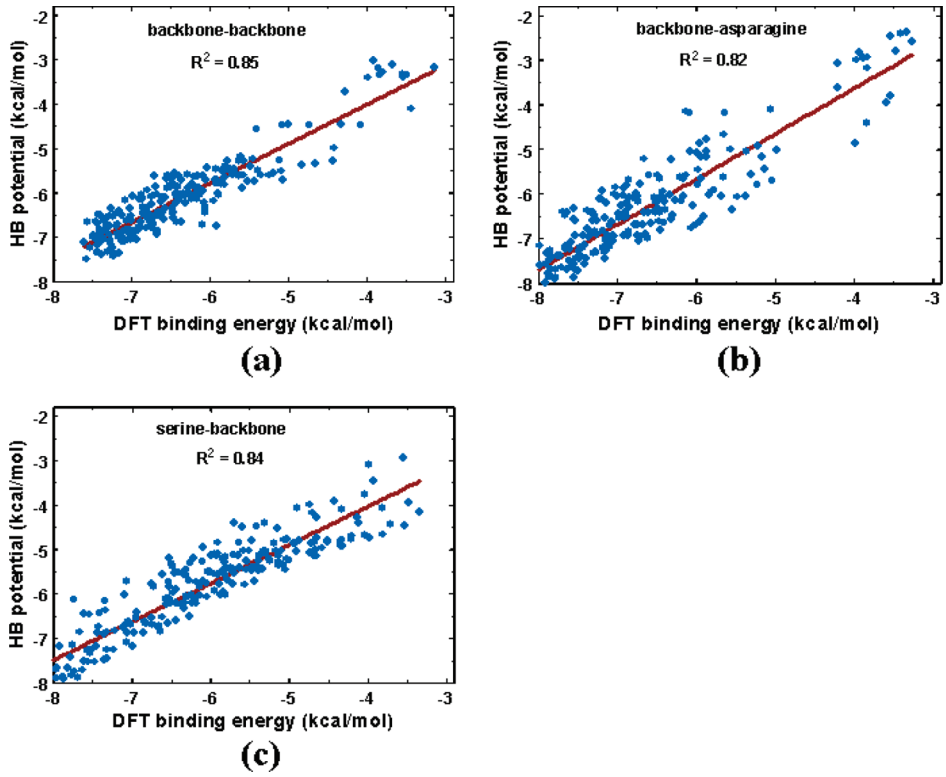

Figure 5. Correlations between the DFT binding energies versus the HB potential energies for (a) Bck−Bck, (b) Bck−Asn, and (c) Ser−Bck HBs.

the charge transfer from the nonbonding orbital of the acceptor atom to the σ^* molecular orbital of the donor group. The involvement of such a covalent character has been well-appreciated in various types of HB.[47] Furthermore, new structural variables other than the two HB angles are required in order to reflect the radial dependence of the angular term. R_θ and R_ϕ can in this regard be the alternative angular variables because they increase and decrease in the same way as the HB distance. Thus, the superiority of the present angular term to the trigonometric functions in modeling the HBs can be attributed to the proper description of the radial dependence of the angular term with the Morse function with respect to the distance-dependent angular variables.

Conclusions

On the basis of DFT calculations and the optimization of the parameters, we have proposed the new angle-dependent potential energy functions for the three types of HBs abundant at the interface of PPI. The new potential functions are constructed by the product of the radial and the angular Morse functions, the latter of which is expressed with respect to the new angular variables: the interatomic distance between the donor and the acceptor atoms (R_θ), and that between the hydrogen atom and the base atom of the acceptor (R_ϕ). Consistent with the significant angular dependence of HBs, the angular part of the new potential functions is found to be comparable in the magnitude of energy values to the radial one. The binding energies of the HBs calculated with the new potential function compare well with those obtained by high-level DFT calculations. The associated R^2 values amount to 0.85, 0.82, and 0.84 for Bck−Bck, Bck−Asn, and Ser−Bck HBs, respectively. The new energy functions are thus expected to find their way as a new potential function for HB in modeling the protein−protein interactions.

Acknowledgment. This work was supported by Grant M1071130000208M113000210 from Pioneer Research Program for Converging Technology of Korea Science and Engineering Foundation.

References and Notes

(1) Pawson, T.; Nash, P. *Science* **2003**, *300*, 445–452.
(2) Fields, S.; Song, O. *Nature* **1989**, *340*, 245–246.
(3) Gavin, A. C.; Bösche, M.; Krause, R.; Grandi, P.; Marzioch, M.; Bauer, A.; Schultz, J.; Rick, J. M.; Michon, A. M.; Cruciat, C. M.; Remor, M.; Höfert, C.; Schelder, M.; Brajenovic, M.; Ruffner, H.; Merino, A.; Klein, K.; Hudak, M.; Dickson, D.; Rudi, T.; Gnau, V.; Bauch, A.; Bastuck, S.; Huhse, B.; Leutwein, C.; Heurtier, M. A.; Copley, R. R.; Edelmann, A.; Querfurth, E.; Rybin, V.; Drewes, G.; Raida, M.; Bouwmeester, T.; Bork, P.; Seraphin, B.; Kuster, B.; Neubauer, G.; Superti-Furga, G. *Nature* **2002**, *415*, 141–147.
(4) Zhu, H.; Bilgin, M.; Bangham, R.; Hall, D.; Casamayor, A.; Bertone, P.; Lan, N.; Jansen, R.; Bidlingmaier, S.; Houfek, T.; Mitchell, T.; Miller, P.; Dean, R. A.; Gerstein, M.; Snyder, M. *Science* **2001**, *293*, 2101–2105.
(5) Bader, G. D.; Hogue, C. W. B. *Bioinformatics* **2000**, *16*, 465–477.
(6) Xenarios, I.; Salwinski, L.; Duan, X. J.; Higney, P.; Kim, S. M.; Eisenberg, D. *Nucleic Acids Res.* **2002**, *30*, 303–305.
(7) Zanzoni, A.; Montecchi-Palazzi, L.; Quondam, M.; Ausiello, G.; Helmer-Citterich, M.; Cesareni, G. *FEBS Lett.* **2002**, *513*, 135–140.
(8) Ng, S. K.; Zhang, Z.; Tan, S. H. *Bioinformatics* **2003**, *19*, 923–929.
(9) Nye, T. M. W.; Berzuini, C.; Gilks, W. R.; Babu, M. M.; Teichmann, S. A. *Bioinformatics* **2005**, *21*, 993–1001.
(10) Chen, W.; Gordon, M. S. *J. Phys. Chem.* **1996**, *100*, 14316–14328.
(11) Umeyama, H.; Morokuma, K. *J. Am. Chem. Soc.* **1977**, *99*, 1316–1332.
(12) Morozov, A. V.; Kortemme, T.; Tsemekhman, K.; Baker, D. *Proc. Natl. Acad. Sci. U.S.A.* **2004**, *101*, 6946–6951.
(13) Isaacs, E. D.; Shukla, A.; Platzman, P. M.; Hamann, D. R.; Barbiellini, B.; Tulk, C. A. *Phys. Rev. Lett.* **1999**, *82*, 600–603.
(14) Dahiyat, B. I.; Gordon, D. B.; Mayo, S. L. *Protein Sci.* **1997**, *6*, 1333–1337.
(15) Bolon, D. N.; Marcus, J. S.; Ross, S. A.; Mayo, S. L. *J. Mol. Biol.* **2003**, *329*, 611–622.
(16) Morris, G. M.; Goodsell, D. S.; Halliday, R. S.; Huey, R.; Hart, W. E.; Belew, R. K.; Olson, A. J. *J. Comput. Chem.* **1998**, *19*, 1639–1662.

(17) Kroon, J.; Kanters, J. A. *Nature* **1974**, *248*, 667–669.
(18) Baker, E. N.; Hubbard, R. E. *Prog. Biophys. Mol. Biol.* **1984**, *44*, 97–179.
(19) Vedani, A.; Dunitz, J. D. *J. Am. Chem. Soc.* **1985**, *107*, 7653–7658.
(20) Kortemme, T.; Morozov, A. V.; Baker, D. *J. Mol. Biol.* **2003**, *326*, 1239–1259.
(21) Fabiola, F.; Bertram, R.; Korostelev, A.; Chapman, M. S. *Protein Sci.* **2002**, *11*, 1415–1423.
(22) McDonald, I. K.; Thornton, J. M. *J. Mol. Biol.* **1994**, *238*, 777–793.
(23) Gavezzotti, A.; Filippini, G. *J. Phys. Chem.* **1994**, *98*, 4831–4837.
(24) Taylor, R.; Kennard, O.; Versichel, W. *J. Am. Chem. Soc.* **1983**, *105*, 5761–5766.
(25) Choi, H.; Kang, H.; Park, H. *J. Comput. Chem.* **2010**, *31*, DOI: 10.1002/jcc.21378.
(26) Lommerse, J. P. M.; Price, S. L.; Taylor, R. *J. Comput. Chem.* **1997**, *18*, 757–774.
(27) Xu, D.; Tsai, C. J.; Nussinov, R. *Protein Eng.* **1997**, *10*, 999–1012.
(28) Kang, Y. K. *J. Phys. Chem. B* **2000**, *104*, 8321–8326.
(29) Morse, P. M. *Phys. Rev.* **1929**, *34*, 57–64.
(30) Grzybowski, B. A.; Ishchenko, A. V.; DeWitte, R. S.; Whitesides, G. M.; Shakhnovich, E. I. *J. Phys. Chem.* **2000**, *104*, 7293–7298.
(31) Schmidt, M. W.; Baldridge, K. K.; Boatz, J. A.; Elbert, S. T.; Gordon, M. S.; Jensen, J. H.; Koseki, S.; Matsunaga, N.; Nguyen, K. A.; Su, S.; Windus, T. L.; Dupuis, M.; Montgomery, J. A. *J. Comput. Chem.* **1993**, *14*, 1347–1363.
(32) Becke, A. D. *J. Chem. Phys.* **1993**, *98*, 5648–5652.
(33) Lee, C.; Yang, W.; Parr, R. G. *Phys. Rev. B* **1988**, *37*, 785–789.
(34) Vargas, R.; Garza, J.; Friesner, R. A.; Stern, H.; Hay, B. P.; Dixon, D. A. *J. Phys. Chem. A* **2001**, *105*, 4963–4968.
(35) Boys, S. F.; Bernardi, F. *Mol. Phys.* **1970**, *19*, 553–566.
(36) MacKerell, A. D., Jr.; Bashford, D.; Bellott, R. L.; Dunbrack, R. L., Jr.; Evanseck, J. D.; Field, M. J.; Fischer, S.; Gao, J.; Guo, H.; Ha, S.; Joseph-McCarthy, D.; Kuchnir, L.; Kuczera, K.; Lau, F. T. K.; Mattos, C.; Michnick, S.; Ngo, T.; Nguyen, D. T.; Prodhom, B.; Reiher, W. E., III; Roux, B.; Schlenkrich, M.; Smith, J. C.; Stote, R.; Straub, J.; Watanabe, M.; Wiorkiewicz-Kuczera, J.; Yin, D.; Karplus, M. *J. Phys. Chem. B* **1998**, *102*, 3586–3616.
(37) Jeffrey, G. A. *An Introduction to Hydrogen Bonding*; Oxford University Press: Oxford; 1997.
(38) Levenberg, K. *Q. Appl. Math.* **1944**, *2*, 164–168.
(39) Marquardt, D. *SIAM J. Appl. Math.* **1963**, *11*, 431–441.
(40) Nooren, I. M.; Thornton, J. M. *EMBO J.* **2003**, *22*, 3486–3492.
(41) Hasegawa, M.; Noda, H. *Nature* **1975**, *254*, 212.
(42) Taylor, R.; Kennard, O. *Acc. Chem. Res.* **1984**, *17*, 320–325.
(43) Platts, J. A.; Howard, S. T.; Bracke, B. R. F. *J. Am. Chem. Soc.* **1996**, *118*, 2726–2733.
(44) Ippolito, J. A.; Alexander, R. S.; Christianson, D. W. *J. Mol. Biol.* **1990**, *215*, 457–471.
(45) Stickle, D. F.; Presta, L. G.; Dill, K. A.; Rose, G. D. *J. Mol. Biol.* **1992**, *226*, 1143–1159.
(46) Ireta, J.; Neugebauer, J.; Scheffler, M. *J. Phys. Chem. A* **2004**, *108*, 5692–5698.
(47) Dash, N.; Chipem, F. A. S.; Swaminathan, F. A. R.; Krishnamoorthy, F. A. G. *Chem. Phys. Lett.* **2008**, *460*, 119–124.

JP909983Y